

# Photophysics of uracil: an explicit time-dependent generating function based method combining both the nonadiabatic and spin-orbit coupling effects

## Supporting Information

Pijush Karak, Torsha Moitra, Kenneth Ruud\*, Swapan Chakrabarti\*  
email: kenneth.ruud@uit.no, swcchem@caluniv.ac.in

### Contents

1	Coordinates of the optimized geometries	S2
2	Normal mode frequencies	S5
3	Position of the singlet and triplet energy levels in eV at CASSCF method.	S6
4	Displacement vectors of a few selected normal modes of the S <sub>2</sub> -non-planar state having dominant contribution to the NACMEs between two different singlet or triplet levels.	S10
5	Potential energy surfaces of a few selected normal modes	S11
6	Normal mode specific internal conversion rate constants.	S12
7	Linear interpolation between S <sub>2</sub> and S <sub>2</sub> -S <sub>1</sub> conical intersection (CI) geometry at the MS-CASPT2 method	S13
8	Variation of k <sub>IC</sub> in s <sup>-1</sup> with energy gap in eV at CASSCF method.	S13
9	Internal conversion rate constants between the singlet or triplet levels at the CASSCF(14e,10o) level of theory	S14
10	Displacement vectors and Duschinsky rotation matrices	S14

# 1 Coordinates of the optimized geometries

The ground ( $S_0$  and  $T_1$ ) as well as the excited states ( $S_1$ ,  $S_2$ (nonplanar),  $S_3$  and  $T_2$ ) were optimized using Gaussian16 software at the b3lyp/6-311g(d,p) level of theory. The  $S_2$ (planar) geometry was optimized at the EOMCCSD/aug-cc-pVDZ method and then the computation of frequencies on that geometry was performed using b3lyp/6-311g(d,p) level of theory.

## $S_0$ geometry ( $\text{\AA}$ )

C	-0.00265	1.70623	-0.00002
N	0.03200	-0.98737	-0.00100
C	-1.22403	-0.40708	-0.00005
C	1.29335	-0.34939	0.00003
C	1.20320	1.10676	-0.00026
N	-1.17303	0.98699	0.00014
H	-2.0705	1.44675	0.00085
H	-0.11976	2.78267	-0.00006
O	-2.26452	-1.02451	0.00038
H	0.04529	-1.99933	-0.00088
H	2.12235	1.67196	-0.00030
O	2.31335	-1.0053	0.00065

## $S_1$ geometry ( $\text{\AA}$ )

C	0.032740	1.757817	-0.000175
N	-0.060502	-0.985326	0.000222
C	1.216860	-0.396503	-0.000060
C	-1.247574	-0.259245	0.000141
C	-1.215897	1.108750	-0.000022
N	1.193200	0.967383	-0.000186
H	2.104323	1.398991	-0.000396
H	0.168423	2.824454	-0.000179
O	2.218547	-1.080260	-0.000167
H	-0.077194	-1.993824	0.000147
H	-2.136715	1.669525	-0.000033
O	-2.306609	-1.049547	0.000281

## $S_2$ non-planar geometry ( $\text{\AA}$ )

C	0.009522	1.757763	0.103009
N	-0.003620	-0.921013	0.383717
C	1.164930	-0.359868	0.032357
C	-1.321598	-0.293532	0.030373
C	-1.225217	1.104324	-0.004919
N	1.190697	0.968118	-0.123935
H	2.007938	1.351040	-0.578555
H	0.168592	2.777659	0.414025
O	2.202672	-1.079883	-0.135253
H	-0.004408	-1.928775	0.495917
H	-2.141102	1.662010	-0.157191
O	-2.215971	-1.100591	-0.234446

S<sub>2</sub> planar geometry (Å)

C	-0.009792	-1.796899	-0.000000
N	-0.000000	1.033774	0.000000
C	-1.202487	0.399608	-0.000000
C	1.289343	0.371462	0.000000
C	1.265720	-1.048198	0.000000
N	-1.128638	-1.028809	-0.000000
H	-2.055757	-1.452678	-0.000000
H	-0.120795	-2.879872	-0.000000
O	-2.317409	0.913143	-0.000000
H	0.005084	2.047878	0.000000
H	2.212593	-1.587931	0.000000
O	2.292738	1.122107	0.000000

S<sub>3</sub> geometry (Å)

C	0.031279	1.765075	-0.068155
N	-0.033404	-0.986934	-0.009409
C	1.157288	-0.382881	0.007636
C	-1.292277	-0.283762	0.002174
C	-1.206805	1.103515	-0.004822
N	1.208248	0.944996	0.019757
H	2.121954	1.365086	-0.036040
H	0.183479	2.785321	0.248852
O	2.256388	-1.062632	0.000482
H	-0.070877	-1.995075	0.000165
H	-2.127332	1.665772	0.011932
O	-2.314893	-1.029770	0.009724

T<sub>1</sub> geometry (Å)

C	0.118839	1.764810	0.234955
N	-0.064959	-0.979118	0.246411
C	1.187978	-0.438929	0.001387
C	-1.295728	-0.313282	0.009016
C	-1.187396	1.109579	-0.069956
N	1.193625	0.953043	-0.110231
H	2.115503	1.340610	-0.258420
H	0.258733	2.826836	0.098356
O	2.201087	-1.094477	-0.105471
H	-0.102853	-1.989338	0.264597
H	-2.043490	1.666277	-0.425517
O	-2.334925	-0.954889	-0.105115

T<sub>2</sub> geometry (Å)

C	0.013514	1.752768	-0.000155
N	-0.045304	-0.994018	0.000419
C	1.221110	-0.394703	-0.000046
C	-1.240040	-0.271686	0.000143

C	-1.217526	1.099866	-0.000062
N	1.187139	0.973756	-0.000154
H	2.093724	1.413267	-0.000505
H	0.137630	2.821188	-0.000144
O	2.233562	-1.061519	-0.000260
H	-0.048461	-2.002071	0.000086
H	-2.142344	1.655487	-0.000132
O	-2.320529	-1.046419	0.000206

T<sub>3</sub> geometry (Å)

C	0.076019	1.759496	-0.000125
N	-0.073030	-0.965530	0.000272
C	1.230858	-0.386587	-0.000038
C	-1.334025	-0.249681	0.000121
C	-1.183636	1.139099	-0.000016
N	1.240459	0.950156	-0.000157
H	2.154591	1.375434	-0.000480
H	0.241337	2.821330	0.000044
O	2.199354	-1.145744	-0.000231
H	-0.116071	-1.980836	0.000415
H	-2.079305	1.742399	-0.000032
O	-2.337836	-1.032339	0.000179

## 2 Normal mode frequencies

S <sub>0</sub>	S <sub>1</sub>	S <sub>2</sub>	S <sub>3</sub>	T <sub>2</sub>	T <sub>1</sub>	T <sub>3</sub>
149.39	103.48	117.90	154.82	93.45	119.74	69.19
167.92	179.21	181.60	242.11	147.42	172.16	204.74
388.55	255.52	286.88	333.65	302.82	213.99	223.14
397.34	341.22	328.96	350.15	334.64	379.02	348.12
521.29	356.27	350.66	416.82	381.60	470.96	352.14
542.59	386.51	474.27	452.73	385.62	498.75	469.34
560.59	498.16	485.20	516.66	494.20	518.08	504.80
570.32	534.74	514.95	532.06	502.90	536.35	513.64
687.48	542.71	548.43	554.45	528.76	546.30	550.72
733.03	555.63	610.87	570.33	560.72	597.82	581.34
768.38	605.19	683.34	621.95	562.50	647.72	615.96
773.78	732.57	756.57	761.24	738.11	716.23	748.70
820.75	753.45	765.08	771.82	775.80	746.23	765.64
962.89	780.78	773.77	782.61	794.66	764.85	774.75
972.44	945.93	880.11	966.96	947.37	933.14	830.75
991.32	1010.87	967.26	980.37	1004.41	959.21	945.58
1085.18	1037.54	1048.11	1055.75	1045.73	1009.20	995.09
1187.11	1141.90	1152.72	1160.22	1150.49	1142.96	1054.57
1225.24	1216.36	1182.00	1264.25	1236.24	1234.69	1159.55
1381.46	1268.89	1314.83	1332.47	1283.78	1356.66	1275.01
1405.07	1356.55	1359.69	1399.10	1363.02	1387.99	1323.28
1420.50	1427.51	1398.97	1421.85	1428.96	1397.41	1374.88
1502.41	1445.95	1432.89	1464.84	1477.41	1416.89	1420.50
1675.98	1486.60	1505.41	1544.62	1487.78	1480.09	1523.03
1789.30	1653.55	1617.88	1667.48	1618.76	1625.29	1658.43
1826.93	1805.28	2243.14	2537.95	1813.84	1795.11	1926.49
3199.54	3242.38	3183.29	3214.95	3235.93	3213.54	3228.24
3242.67	3278.50	3229.85	3238.55	3273.58	3223.93	3282.44
3600.59	3641.27	3581.29	3634.10	3647.87	3605.10	3563.66
3641.67	3644.15	3586.71	3652.66	3651.50	3611.31	3643.59

**Table S1.** Frequencies( in  $\text{cm}^{-1}$  ) as computed at (u)b3lyp/6-311g(d,p) level of theory using Gaussian16 software.

3 Position of the singlet and triplet energy levels in eV at CASSCF method.

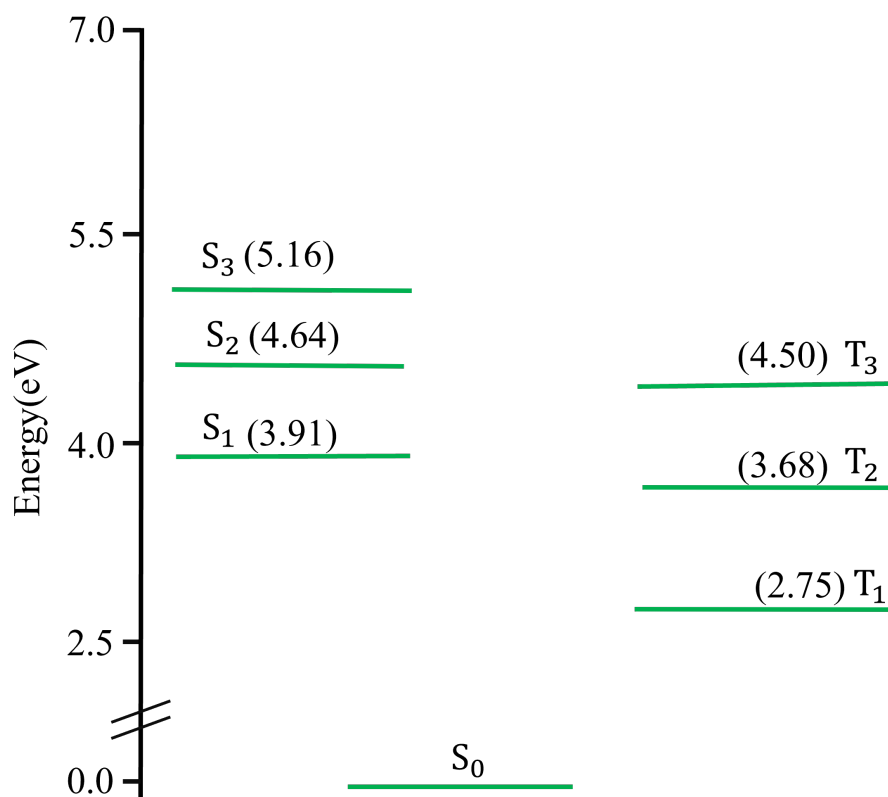


**Fig. S1.** Pictorial representation of the energy levels obtained with the S<sub>2</sub> geometry of uracil at the CASSCF(14e,10o) level of theory. The energy values are in eV given in parenthesis.

## CASSCF orbitals of the singlet and the triplet states computed at the $S_2$ geometry

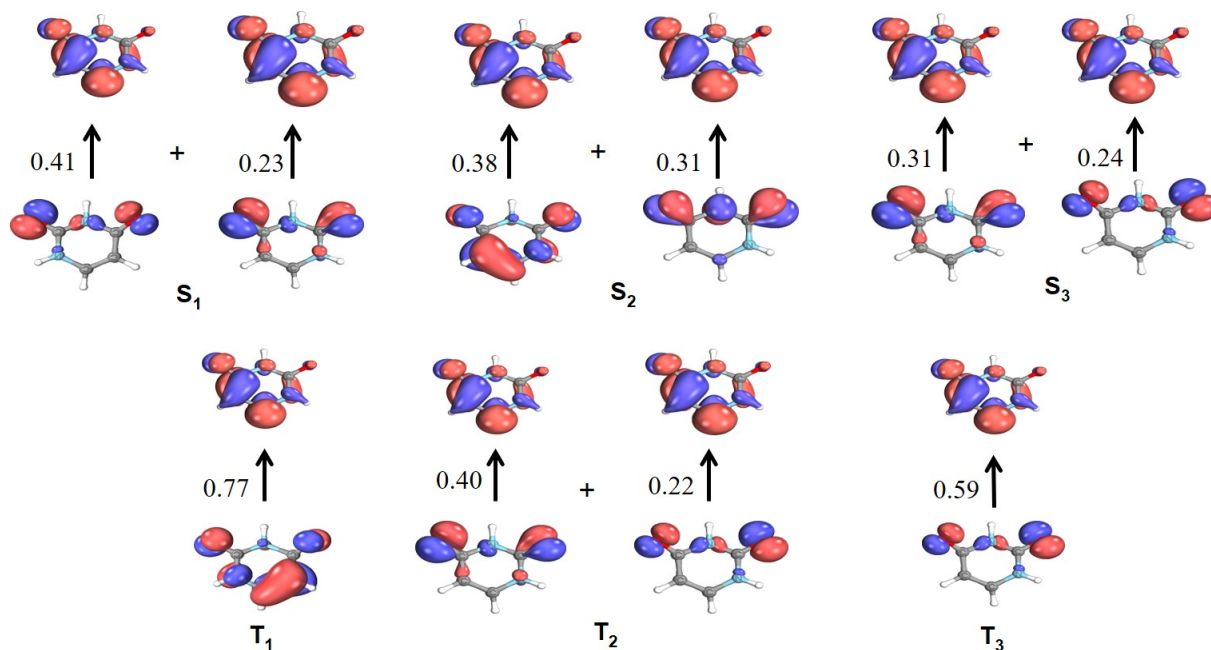


**Fig. S2.** Singlet and triplet electronic state character obtained at CASSCF(14e,10o)/def2-TZVP level of theory using  $S_2$  optimized geometry.

Intersystem crossing between the singlet and triplet states is mainly governed by two important factors, namely, energy gap and SOCME between them. Among them the SOCME in the rate expression appears as a square term and hence it dominates over the energy gap factor. To explain qualitatively, how SOC facilitates ISC, the nature of the orbitals comprising the electronic states involved in the transition should be considered. To study this, we look at the CASSCF orbitals comprising the excited states in Fig.S2. The  $S_1$  electronic state has major contributions from the  $p_z$ ,  $p_x$ ,  $p_y$  atomic orbitals of the  $O_9$  and  $O_{12}$  atoms and also the  $p_z$  orbital of the  $C_1$ ,  $C_4$  and  $C_5$  atoms. In contrast, only the  $p_z$  orbital of the  $O_9$ ,  $O_{12}$ ,  $C_1$  and  $C_5$  atoms has large contributions in the  $T_1$  state. From this picture, we can estimate that the  $\hat{L}_z$  operator connecting the  $p_z$  orbitals of C as well as O atoms of the  $S_1$  and  $T_1$  states and also the  $\hat{L}_{+/-}$  operator coupling the  $p_z$  orbital of  $T_1$  state with that of the  $p_y$  and  $p_x$  orbitals of the  $S_1$  state for both C and O atoms, leads to the significant SOC value of  $53.10 \text{ cm}^{-1}$  between  $S_1$  and  $T_1$  states. Similar analysis is also true for for  $S_3$ - $T_3$ ,  $S_2$ - $T_2$  and  $S_2$ - $T_1$ , which have corresponding SOC of  $56.18$ ,  $19.44$  and  $15.28 \text{ cm}^{-1}$  respectively. The higher values of SOC between  $S_1$ - $T_1$  and  $S_3$ - $T_3$  arise due to the larger contribution of the atomic orbitals ( $p_z$ ,  $p_y$ ,  $p_x$ ) of O and C atoms in the former pathway and contribution of  $p_x$  and  $p_z$  of  $N_2$  in the latter transition.

## Mode specific nonadiabatic coupling vectors (NACMEs)

$\omega_{S_2}(\text{cm}^{-1})$	NACME $_{S_3-S_2}$ (a.u.)	NACME $_{S_2-S_1}$ (a.u.)	NACME $_{T_2-T_1}$ (a.u.)
$\omega_1 = 117.90$	7.76002998E-04	1.48363074E-03	1.58658717E-04
$\omega_2 = 181.60$	3.65964865E-04	5.57537656E-04	2.86894559E-04
$\omega_3 = 286.88$	2.20003352E-03	1.78145000E-03	2.16550427E-03
$\omega_4 = 328.95$	2.01355177E-03	3.46044032E-03	6.31499104E-04
$\omega_5 = 350.66$	5.66056138E-03	1.05705962E-03	7.10672408E-04
$\omega_6 = 474.26$	3.03356373E-03	1.99337373E-03	7.18050636E-04
$\omega_7 = 485.20$	1.94071431E-03	1.19192339E-03	7.22190016E-04
$\omega_8 = 514.95$	8.01453367E-04	2.47899583E-03	4.92417661E-04
$\omega_9 = 548.42$	2.02249037E-03	3.54057108E-03	3.00675689E-04
$\omega_{10} = 610.86$	6.99708296E-04	5.99646801E-03	2.48900591E-03
$\omega_{11} = 683.34$	1.55475701E-03	2.56310729E-03	7.58672133E-04
$\omega_{12} = 756.57$	3.45308450E-03	1.52230030E-04	4.81726660E-04
$\omega_{13} = 765.08$	2.13766447E-03	3.93654360E-03	8.85971713E-06
$\omega_{14} = 773.77$	2.43262039E-03	3.33694229E-03	3.73851867E-06
$\omega_{15} = 880.10$	5.30165248E-03	2.86960183E-03	4.54266672E-04
$\omega_{16} = 967.26$	9.96061368E-04	1.43948375E-04	1.72205939E-04
$\omega_{17} = 1048.10$	2.31651240E-03	4.99785063E-04	1.66662867E-05
$\omega_{18} = 1152.71$	4.91754571E-03	3.72572249E-05	7.81253766E-05
$\omega_{19} = 1182.00$	6.61430124E-04	1.24236406E-03	4.17539792E-04
$\omega_{20} = 1314.82$	4.54468699E-03	4.68172785E-03	9.64349485E-04
$\omega_{21} = 1359.68$	4.42613289E-03	2.07221508E-03	2.42709386E-04
$\omega_{22} = 1398.96$	9.22293693E-04	3.31485673E-04	5.07181045E-04
$\omega_{23} = 1432.89$	1.75175853E-02	3.20402300E-03	2.17730785E-03
$\omega_{24} = 1505.41$	1.10596120E-02	8.03841464E-03	2.02693813E-03
$\omega_{25} = 1617.88$	1.28597207E-02	9.69238952E-03	2.04378885E-04
$\omega_{26} = 2243.13$	1.70365553E-02	2.14493163E-02	1.45300210E-03
$\omega_{27} = 3183.29$	1.62241806E-04	4.11651767E-04	2.95502250E-04
$\omega_{28} = 3229.85$	6.53257652E-04	7.72324333E-04	1.97583242E-04
$\omega_{29} = 3581.29$	3.50671029E-03	3.68964043E-03	3.88095621E-04
$\omega_{30} = 3586.70$	3.87876108E-03	2.73942039E-03	4.56529342E-05

**Table S2.** Magnitude of the normal mode specific nonadiabatic coupling vector elements(NACMEs) in a.u. at the MS-CASPT2 method.

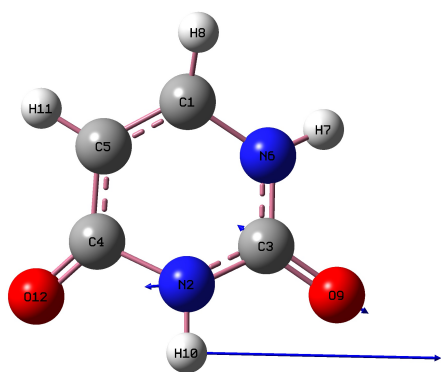


## Mode specific nonadiabatic coupling vectors (NACMEs)

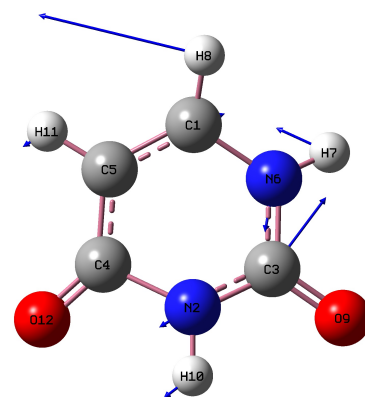
$\omega_{S_2}(\text{cm}^{-1})$	NACME $_{S_3-S_2}$ (a.u.)	NACME $_{S_2-S_1}$ (a.u.)	NACME $_{T_2-T_1}$ (a.u.)
$\omega_1 = 117.90$	1.54766371E-03	9.29847592E-04	4.55901900E-04
$\omega_2 = 181.60$	1.02340989E-03	5.80630498E-04	5.98930579E-04
$\omega_3 = 286.88$	7.28939369E-04	5.20423055E-04	1.41302403E-03
$\omega_4 = 328.95$	2.79358681E-03	7.63351389E-04	3.92654270E-04
$\omega_5 = 350.66$	2.56412255E-04	7.32114888E-04	4.69044084E-04
$\omega_6 = 474.26$	1.37780036E-03	1.06989499E-03	4.05569561E-04
$\omega_7 = 485.20$	1.66766206E-03	5.87386719E-04	3.72241426E-04
$\omega_8 = 514.95$	2.00414052E-03	6.22883672E-04	3.81047605E-04
$\omega_9 = 548.42$	2.57060892E-04	9.13765281E-04	8.54200625E-05
$\omega_{10} = 610.86$	1.03873224E-03	2.06200965E-03	1.76598551E-03
$\omega_{11} = 683.34$	3.91924893E-03	1.84379649E-04	5.61052933E-04
$\omega_{12} = 756.57$	4.05502564E-04	5.43058675E-04	8.25963682E-04
$\omega_{13} = 765.08$	7.54590146E-04	1.41738099E-03	9.38816593E-05
$\omega_{14} = 773.77$	1.05116027E-03	3.75249103E-04	4.22314071E-04
$\omega_{15} = 880.10$	3.89976369E-04	3.77891032E-04	9.61042388E-05
$\omega_{16} = 967.26$	2.03027832E-03	1.15339302E-04	7.45022990E-05
$\omega_{17} = 1048.10$	1.37136655E-03	1.75646448E-03	2.57568900E-06
$\omega_{18} = 1152.71$	2.66946666E-03	2.46330840E-03	1.73045642E-04
$\omega_{19} = 1182.00$	5.05485979E-04	7.55292829E-04	2.27730314E-04
$\omega_{20} = 1314.82$	2.02403706E-03	1.46492047E-03	7.84475356E-04
$\omega_{21} = 1359.68$	8.25345982E-04	1.06079294E-03	9.81510238E-05
$\omega_{22} = 1398.96$	3.90865328E-03	3.39966246E-05	1.11657382E-05
$\omega_{23} = 1432.89$	4.98720584E-03	7.20016367E-04	2.12274434E-04
$\omega_{24} = 1505.41$	6.95940945E-03	2.01314013E-03	1.06031192E-03
$\omega_{25} = 1617.88$	7.82380719E-03	2.99172313E-03	6.79792895E-04
$\omega_{26} = 2243.13$	1.29351104E-02	1.07276207E-02	2.70361919E-03
$\omega_{27} = 3183.29$	2.61915149E-04	2.93150573E-04	2.05844539E-04
$\omega_{28} = 3229.85$	2.09113423E-04	1.42673263E-04	5.65051087E-05
$\omega_{29} = 3581.29$	1.07411388E-03	1.90662162E-03	3.27802933E-04
$\omega_{30} = 3586.70$	2.14625616E-03	6.95662806E-04	1.21082783E-04

**Table S3.** Magnitude of the normal mode specific nonadiabatic coupling vector elements(NACMEs) in a.u. at the CASSCF method.

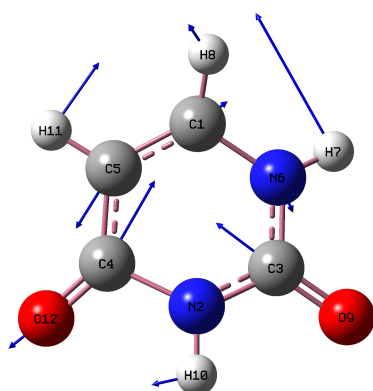
4 Displacement vectors of a few selected normal modes of the  $S_2$ -non-planar state having dominant contribution to the NACMEs between two different singlet or triplet levels.



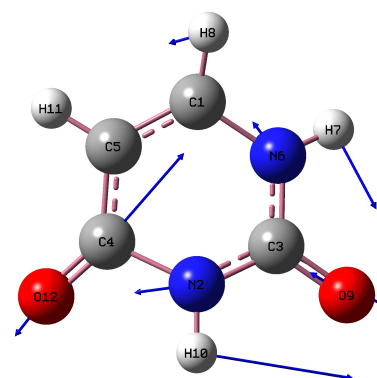
(a)  $\omega_{20} = 1314.82 \text{ cm}^{-1}$



(b)  $\omega_{24} = 1505.41 \text{ cm}^{-1}$



(c)  $\omega_{25} = 1617.88 \text{ cm}^{-1}$



(d)  $\omega_{26} = 2243.13 \text{ cm}^{-1}$

**Fig. S3.** Displacement vector of a few selected normal modes of  $S_2$  geometry having significant NACMEs.

## 5 Potential energy surfaces of a few selected normal modes

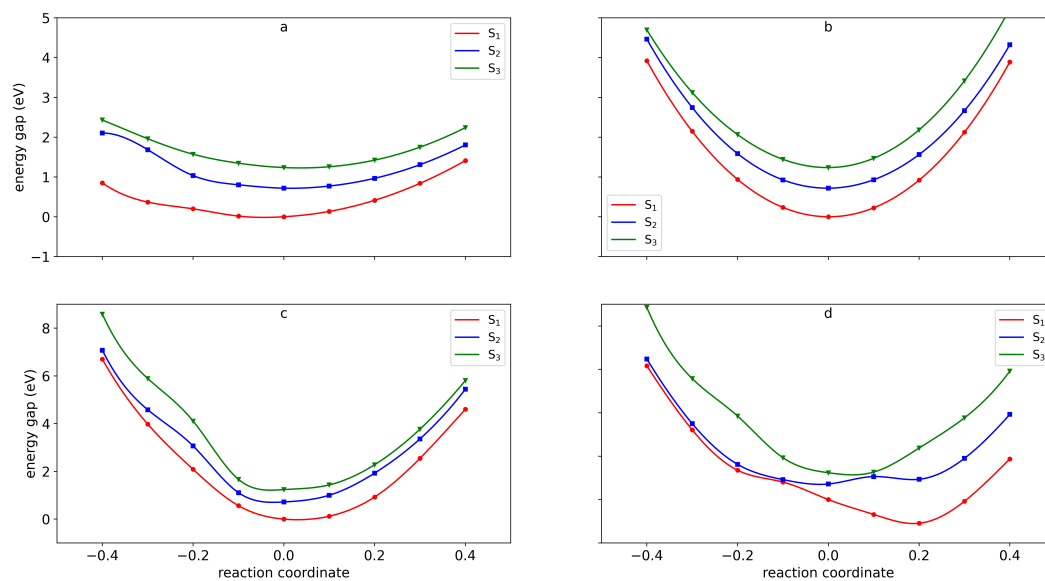


**Fig. S4.** Potential energy surfaces of normal modes obtained using CASSCF/(14e,10o) method. Here the reaction coordinate indicate the manual displacement of the normal mode coordinate along the direction of the displacement vector of the respective normal mode. a, b, c and d denotes the potential energy surface for normal mode 20, 24, 25 and 26 with frequencies 1314, 1505, 1617 and 2243  $\text{cm}^{-1}$ , respectively.

## 6 Normal mode specific internal conversion rate constants.

**Table S4.** Internal conversion(IC) rate constant computed using the energy gap taken from the MS-CASPT2 method obtained at the  $S_2$ -nonplanar geometry of e few selected normal modes having dominant NAC values.

Normal mode	$k_{IC}^{S_3-S_2}$ ( $s^{-1}$ )	$k_{IC}^{S_2-S_1}$ ( $s^{-1}$ )	$k_{IC}^{T_2-T_1}$ ( $s^{-1}$ )
$\omega_{20}$	$3.29 \times 10^{10}$	$6.60 \times 10^9$	$1.94 \times 10^9$
$\omega_{24}$	$2.35 \times 10^{11}$	$1.85 \times 10^{10}$	$1.52 \times 10^{10}$
$\omega_{25}$	$3.45 \times 10^{11}$	$4.40 \times 10^{10}$	$1.42 \times 10^8$
$\omega_{26}$	$9.31 \times 10^{11}$	$2.11 \times 10^{11}$	$9.92 \times 10^9$

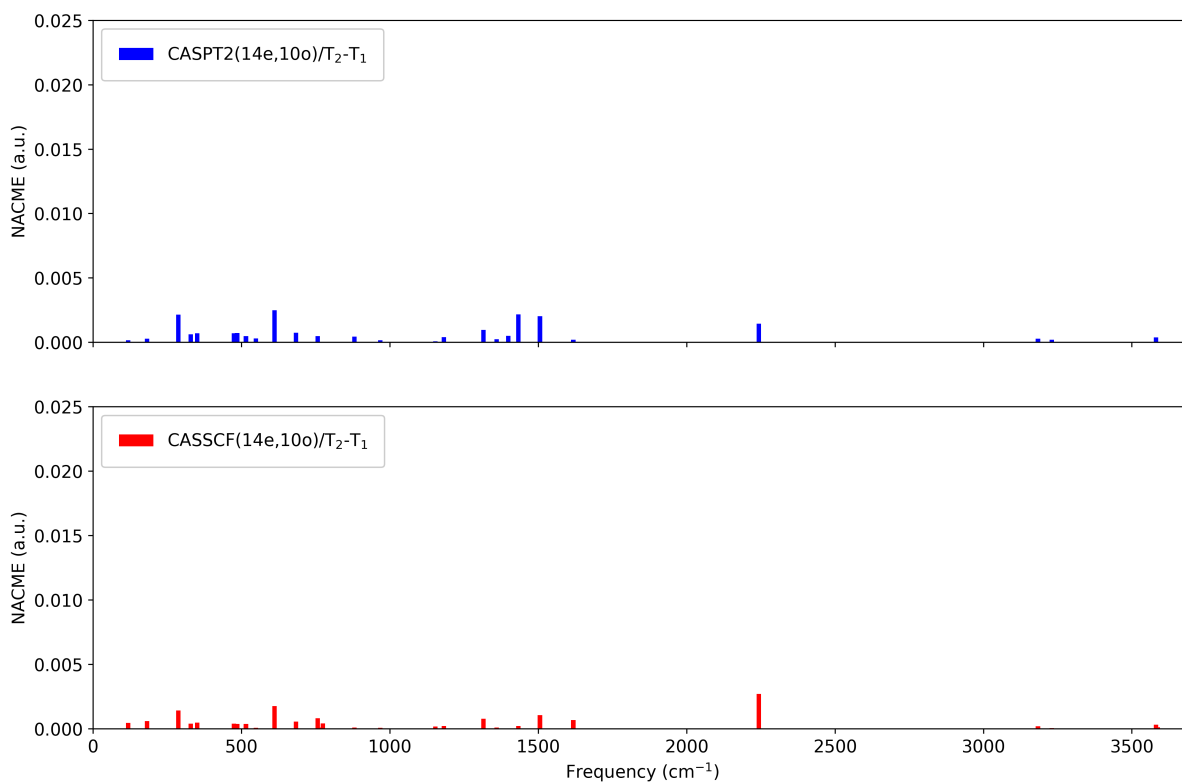


**Fig. S5.** Mode specific NACMEs between the  $T_2$  and  $T_1$  states..

## 7 Linear interpolation between $S_2$ and $S_2$ - $S_1$ conical intersection (CI) geometry at the MS-CASPT2 method

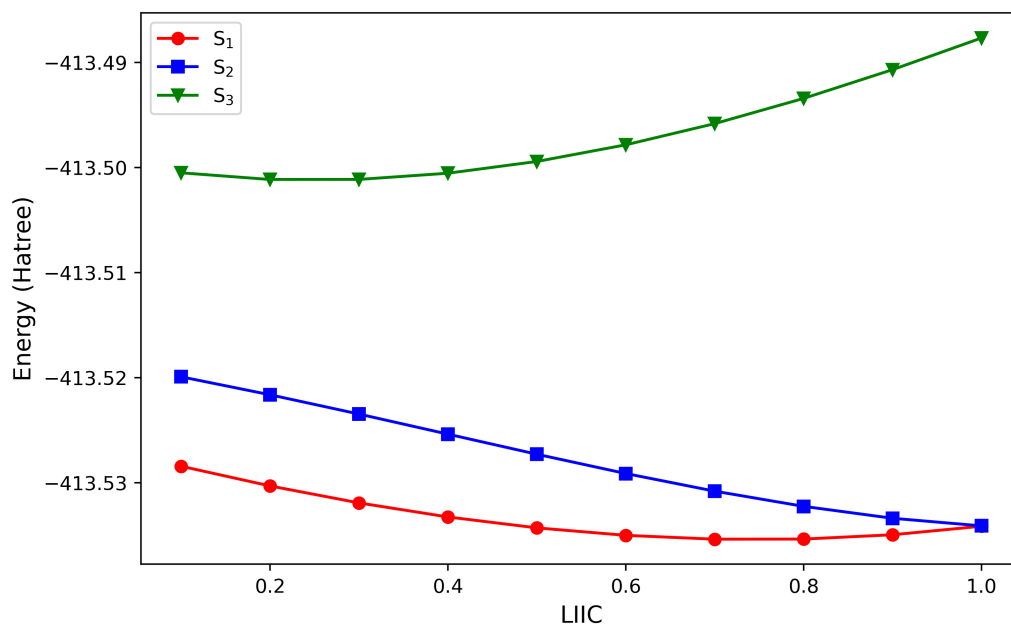


**Fig. S6.** Potential energy surfaces generated by linear interpolation in internal coordinate (LIIC) technique between  $S_2$  and  $S_2$ - $S_1$  conical intersection (CI) geometry at the MS-CASPT2 level of theory using (14e,10o) active space.

## 8 Variation of $k_{IC}$ in $s^{-1}$ with energy gap in eV at CASSCF method.

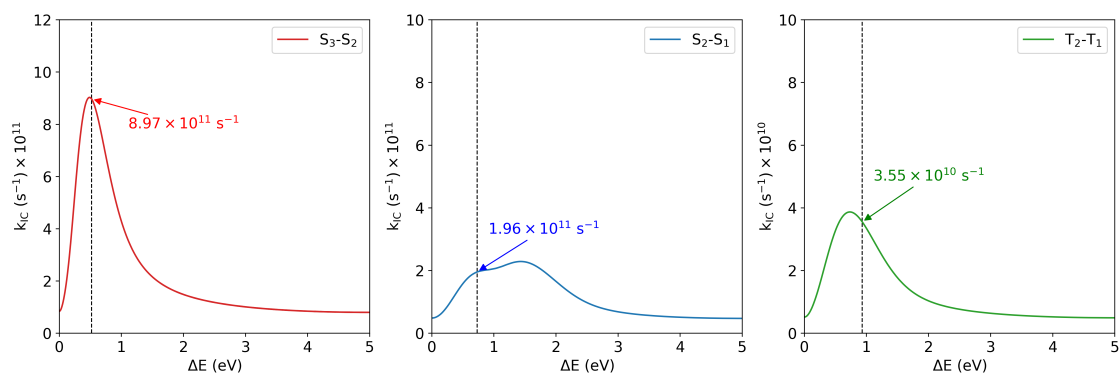


**Fig. S7.** Variation of  $k_{IC}$  with the energy gap obtained by Fourier transforming the generating function.

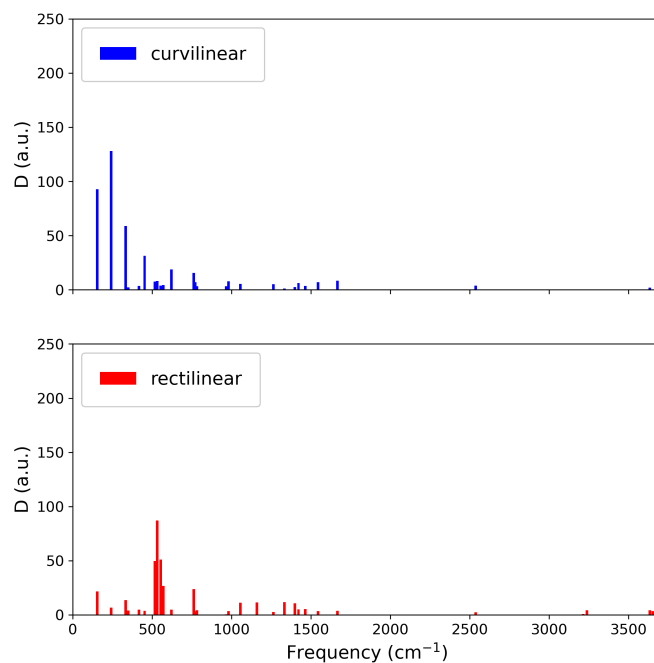
## 9 Internal conversion rate constants between the singlet or triplet levels at the CASSCF(14e,10o) level of theory

**Table S5.** Internal conversion rate constant calculated using the energy gap and NACME obtained at the  $S_2$  geometry using the CASSCF level of theory with (14e,10o) active space. Here a and b denotes the rate constant evaluated involving the J and D computed in curvilinear and rectilinear coordinates, respectively.

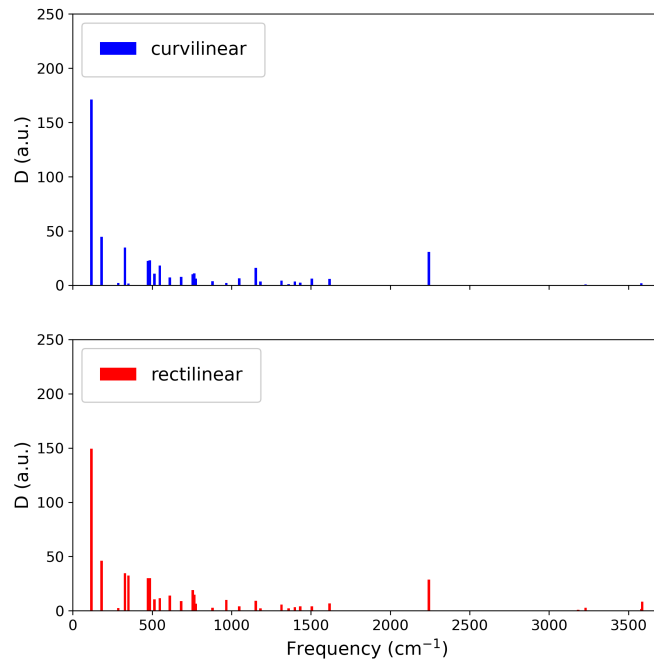
Transition	$\Delta E$ (eV)	norm (Bohr $^{-1}$ )	$k_{IC}^a$ (s $^{-1}$ )	$k_{IC}^b$ (s $^{-1}$ )
$S_3 \rightarrow S_2$	0.52	2.88	$8.97 \times 10^{11}$	$3.73 \times 10^{11}$
$S_2 \rightarrow S_1$	0.73	1.88	$1.96 \times 10^{11}$	$2.20 \times 10^{11}$
$T_2 \rightarrow T_1$	0.93	0.63	$3.55 \times 10^{10}$	$2.70 \times 10^{10}$

## 10 Displacement vectors and Duschinsky rotation matrices

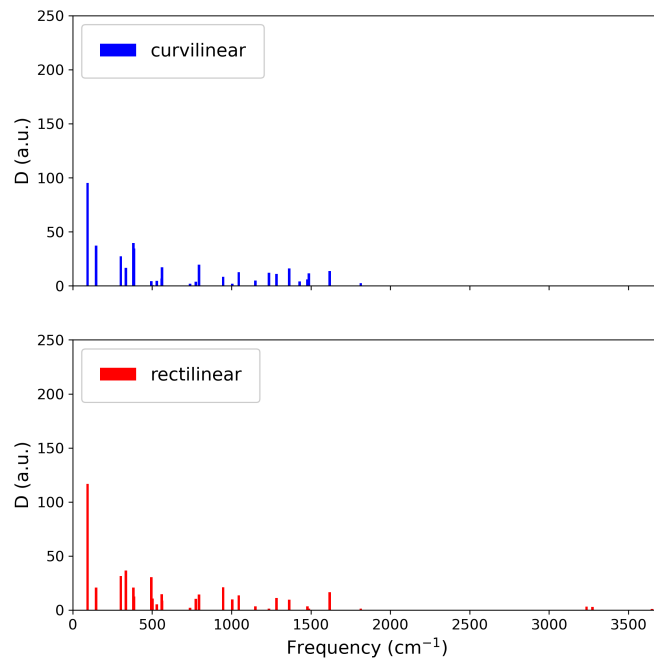
### Displacement vectors



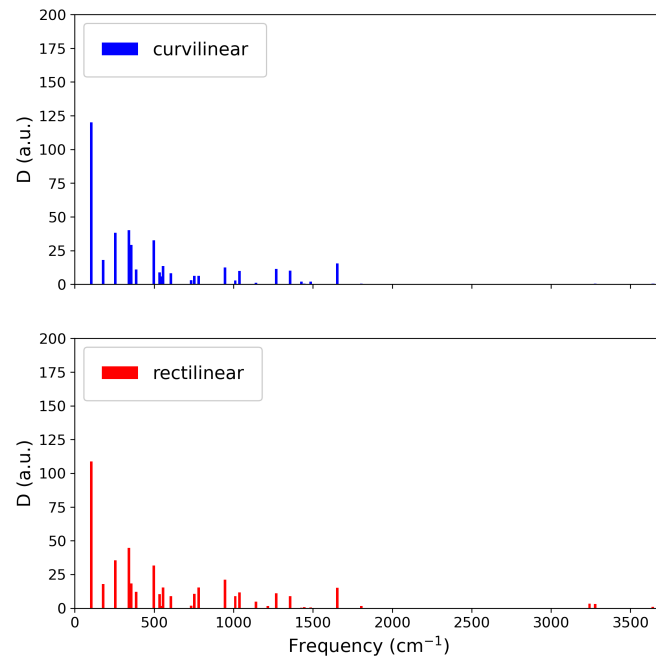
$S_3 \rightarrow S_2$



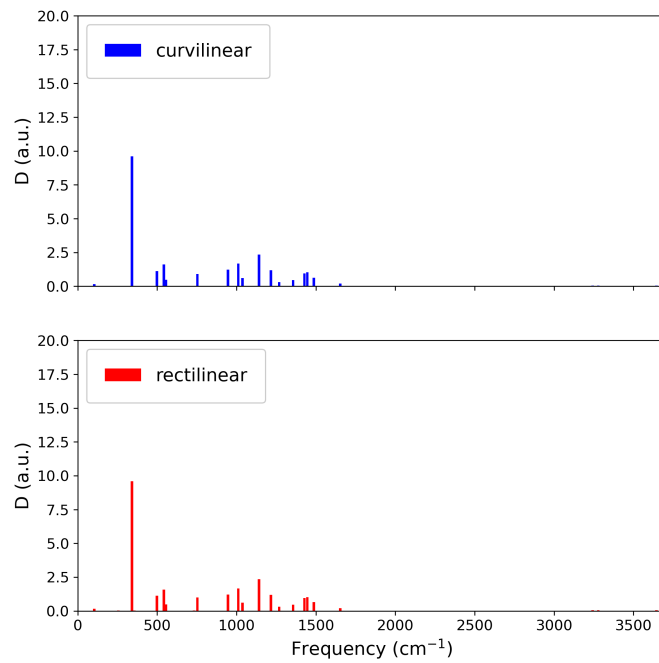
$S_2 \rightarrow S_1$



$T_2 \rightarrow T_1$

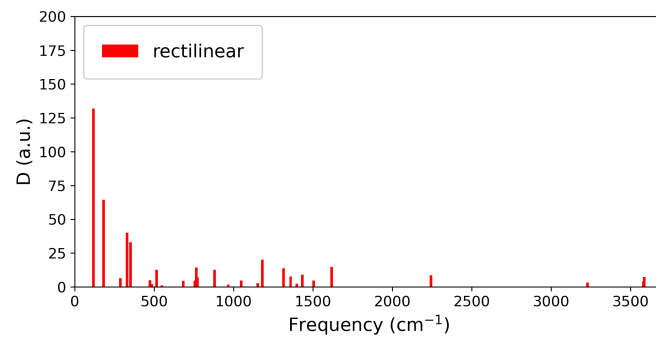
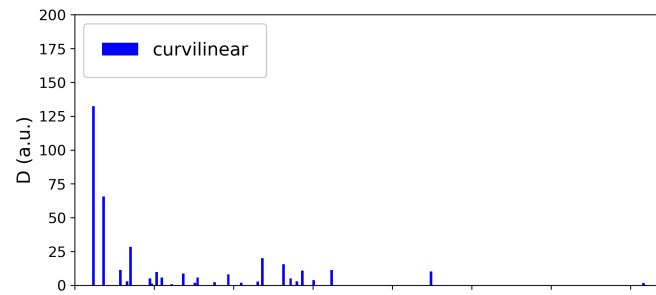


$S_1 \rightarrow T_1$

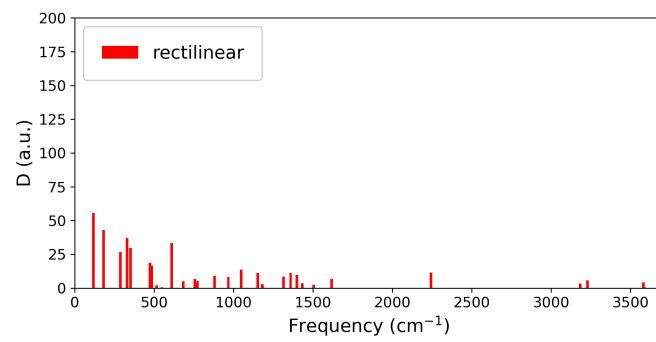
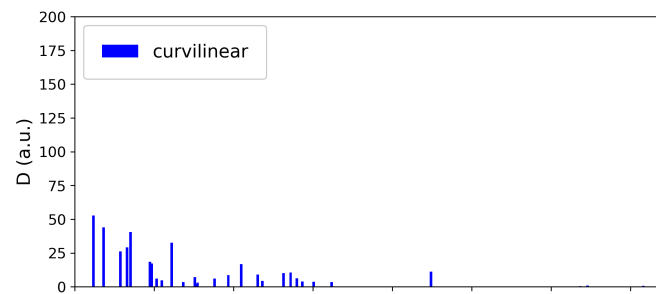


$S_1 \rightarrow T_2$

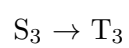
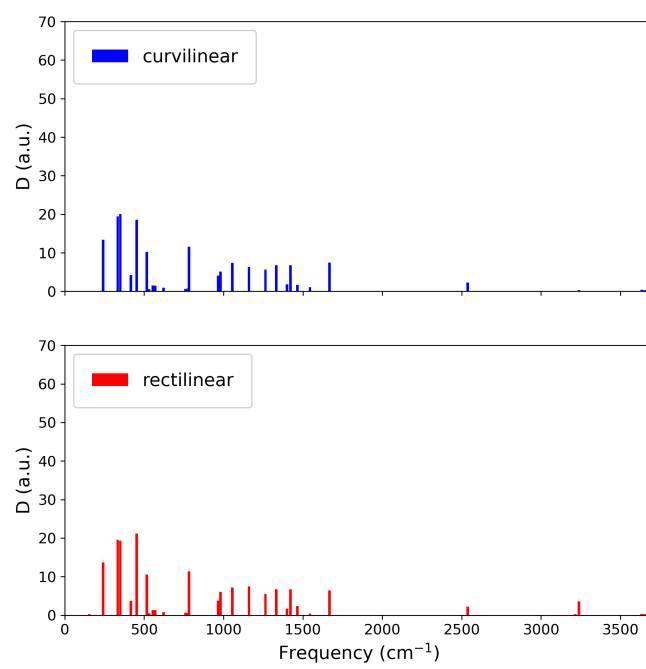




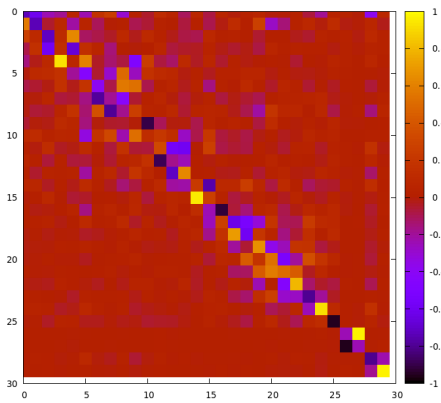
$S_2 \rightarrow T_2$



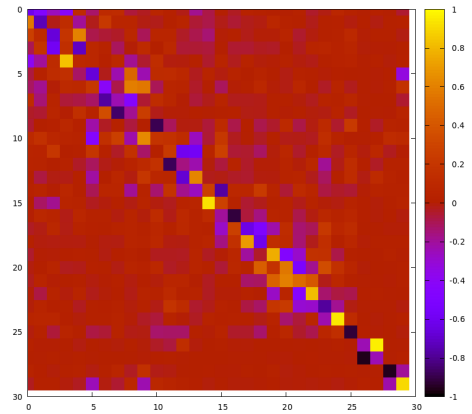
$S_2 \rightarrow T_1$



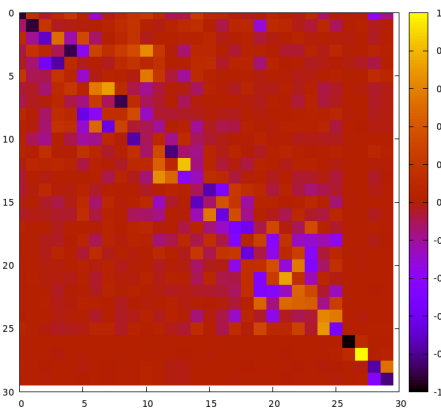
# Duschinsky rotation matrices



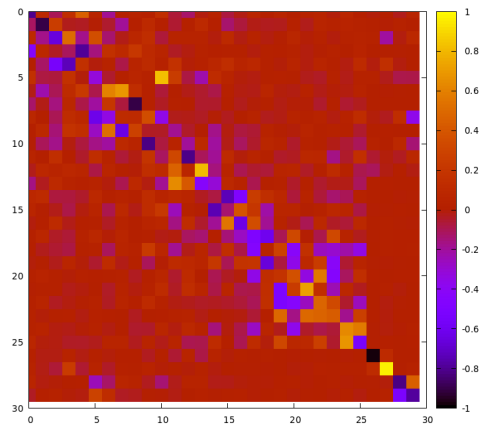
$S_3 \rightarrow S_2$  (curvilinear)



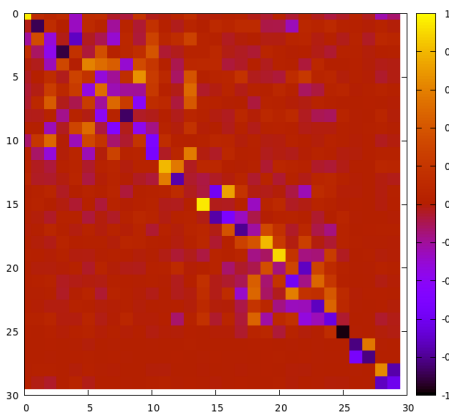
$S_3 \rightarrow S_2$  (rectilinear)



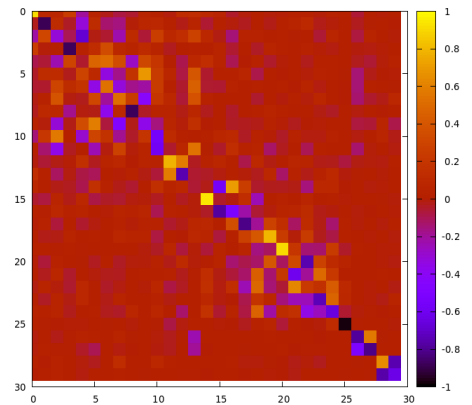
$S_2 \rightarrow S_1$  (curvilinear)



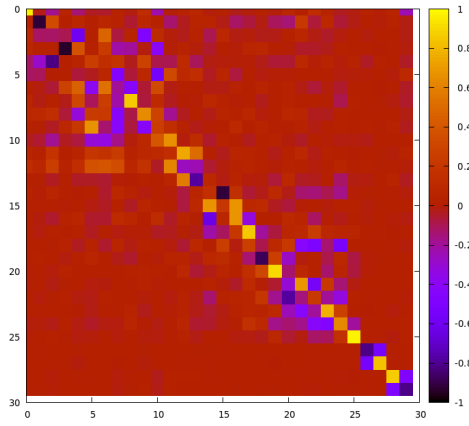
$S_2 \rightarrow S_1$  (rectilinear)



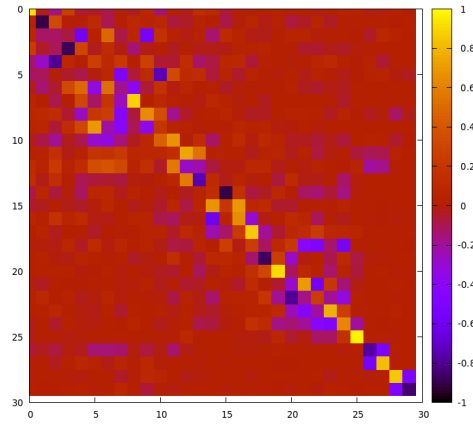
$T_2 \rightarrow T_1$  (curvilinear)



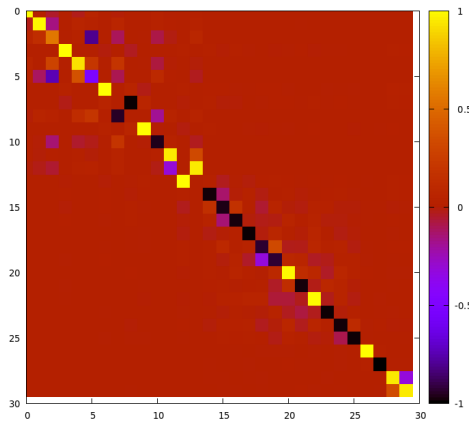
$T_2 \rightarrow T_1$  (rectilinear)



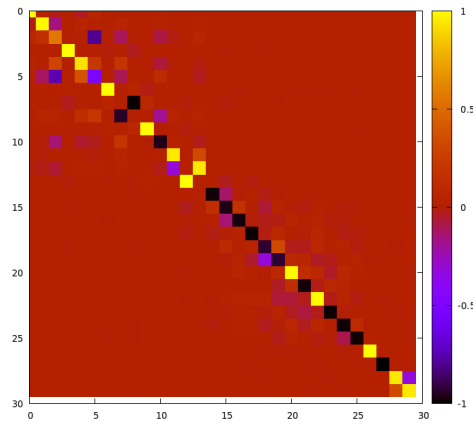
$S_1 \rightarrow T_1$  (curvilinear)



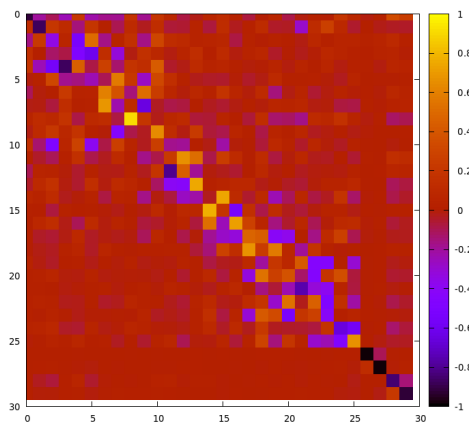
$S_1 \rightarrow T_1$  (rectilinear)



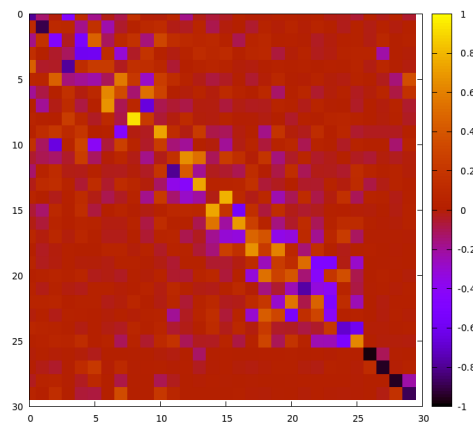
$S_1 \rightarrow T_2$  (curvilinear)



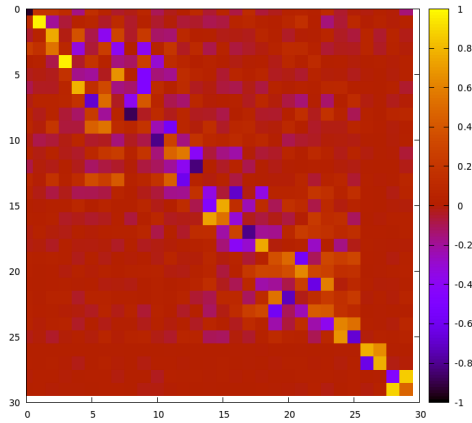
$S_1 \rightarrow T_2$  (rectilinear)



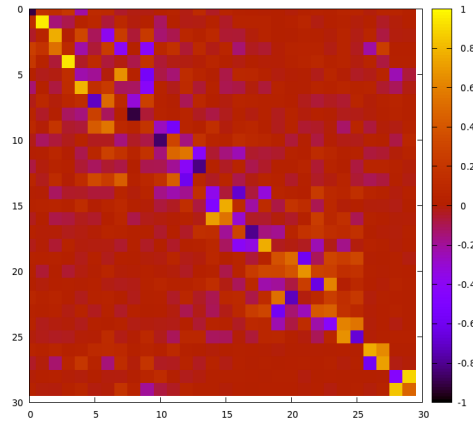
$S_2 \rightarrow T_2$  (curvilinear)



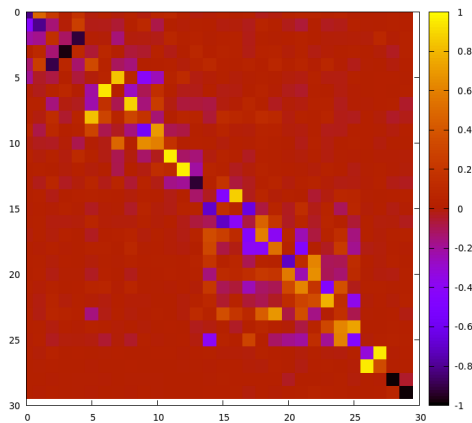
$S_2 \rightarrow T_2$  (rectilinear)



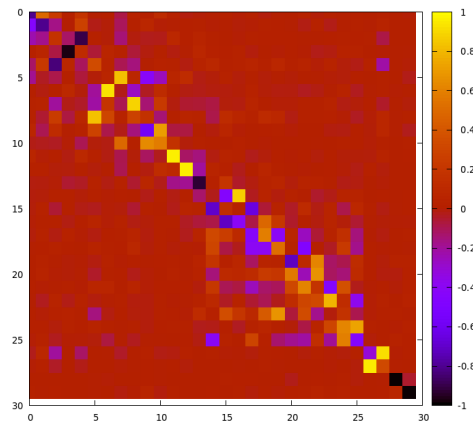
$S_1 \rightarrow T_1$  (curvilinear)



$S_1 \rightarrow T_1$  (rectilinear)



$S_3 \rightarrow T_3$  (curvilinear)



$S_3 \rightarrow T_3$  (rectilinear)